Acta Scientiarum
http://periodicos.uem.br/ojs/acta
ISSN on-line: 1807-8664
Doi: 10.4025/actascitechnol.v47i1.73252

Investigation of The Effect of Borosintering Process on Various Properties of Iron-Based Materials

Lutuf Ertürk* **and Burhan Selçuk**

Department of Mechanical Engineering, Faculty of Engineering, Sivas Cumhuriyet University, Sivas, 58140, Türkiye. *Author for correspondence: E-mail: lutuferturk@cumhuriyet.edu.tr

ABSTRACT. In this study, samples prepared by pressing iron-based powder mixtures were divided into two different groups; sintering and boriding processes were applied in two steps in some of the samples, and in a single step in some of them. Sintering and boriding processes were applied at 950, 1000 and 1050°C for 2 hours. Various properties of borided and unborided samples in the first group and borosintered samples in the second group were compared. The microstructure in the samples was examined by optical microscope and SEM. Elemental analysis was performed by EDX. Phases formed as a result of boriding were detected by XRD. Surface roughness, microhardness measurements and wear tests were conducted on the samples. In the samples produced by powder metallurgy, the specifications of the structures formed as a result of first sintering and then boronizing process were similar. In both cases, the microhardness values of the material increased and wear-resistant structures were formed. It has been observed that the properties of the resulting structures show some changes depending on the temperature.

Keywords: Wear; iron; powder metallurgy; borosintering; boriding; microhardness.

Received on August 04, 2024.
Accepted on March 06, 2025.

Introduction

The popularity of powder metallurgy (PM) can be attributed to its low energy consumption, cheap manufacturing costs, and great benefits. Different sized powders are used for different purposes; they are formed by pressing, heat-treated to increase their strength, and then their qualities are regulated (Altıntaş et al., 2016). PM method are more competitive than other manufacturing methods for a wide range of high flexibility of manufacturing processes. Because PM doesn't require as many machining steps as other methods do for castings and machined semi-products, it offers superior precision (Çavdar et al., 2015). In recent years, PM parts have become more and more common in structural and automotive applications. Higher density, improved mechanical characteristics, and relatively lower processing temperatures are just a few of the benefits that the PM process provides over conventional casting techniques (Kare et al., 2021).

Boriding is a common thermochemical surface hardening method for improving the characteristics and extending the life of both ferrous and non-ferrous materials (Sinha, 1991). Boronizing is typically carried out for 0.5 to 10 hours at temperatures between 800 and 1050°C. Pack boriding is the most widely used boriding process in the industry since it is inexpensive and easy to use (Keddam, & Chentouf, 2005). An activator, a deoxidizer, and a boron source are present in the boronizing media. A single-phase Fe_2B or two-phase (FeB + Fe_2B) structure may form on the material surface, depending on the chemical activity of boron in the boronizing media and the chemical composition of the basis materials. With the boriding process, a multiphase metal boride layer is produced, consisting mostly of Fe_2B and FeB in unalloyed steels and metal borides in alloyed steels. Although FeB has richer boron concentration and higher hardness, it has relatively lower impact resistance and fracture toughness. For this reason, the formation of the Fe_2B phase is more desirable than FeB (Bouarour et al., 2014; Ozbek & Bindal, 2002).

Šalak et al. (2008) applied pack boriding process to steels produced by powder metallurgy in a powder mixture involving of halide-free ferroborane, carbon ferromanganese and alumina. In the study, Fe-C and low alloy Fe-Ni-Mo-(Cu)-C steel tensile bars were sintered in cracked ammonia at 1120°C for 1 hour and then boronized at 1050°C for 2 hours. It has been stated that this boriding process causes the formation of hard

surface layers and further increases the tensile strength with subsequent heat treatment. Özdemir et al. (2009) performed pack boriding process on AISI 316 stainless steel produced by PM in an environment containing Ekabor at 800, 875 and 950°C for 2, 4 and 8 hours. After boriding, it was determined that the main dominant phase was Fe_2B, and the secondary phase was CrB and Ni_2B. It has been stated that the thickness of the boride layer varies between 7 and 87 µm depending on the processing time and temperature. It has been stated that the hardness of the subtrate surface is approximately 180 HV, while the hardness of the boride layer is over 1700 HV. Yılmaz and Varol (2010) applied boriding and shot peening processes to PM steel samples (containing 3% copper, 0.2% C), individually or in combination. It has been stated that surface hardness values such as 1800-2500 HV are obtained after boriding, and this value is considerably higher than the hardness value of the substrate material (200 HV). De Almeida et al. (2018) applied boriding process to AISI M2 steel produced by the PM method. It was stated that the boronized layer thickness was 46.5 ± 5.1 µm and the average hardness was 2162 $HV_{0.025}$. Aksöz et al. (2021) produced samples from pre-alloyed NiTi powders by powder metallurgy method. The samples, pressed under 700 MPa pressure at 300°C, were sintered under a high-purity Argon atmosphere in a high-temperature resistant Quartz glass tube at 1200°C for 120 minutes. For six and twelve hours, sintered samples were boronized at 900 and 1000°C. It was reported that when all of the boriding parameters were used, the samples' surface hardness rose. It was reported that the sample borided at 1000°C for 12 hours had the largest layer thickness (50 µm) and the highest hardness value (2074.9 HV). Kayalı and Yönetken (2021) produced samples with different volumetric compositions consisting of Fe-Mn-Cr. In order to improve the lifespan of PM ceramic-metal composites, a pack boronizing process was implemented, which needed 4 hours at 950°C. According to the report, depending on their composition, the unborided samples' hardness values ranged from 47.5 to 240.6 HV0.05 and the boronized samples' hardness values from 1641 to 1950 HV0.05. It was mentioned that the ball on disc method was used for the dry sliding wear testing (slide speed: 0.3 m s^{-1}, load: 5 N, distance: 250 m). The Daimler-Benz Rockwell-C adhesion test was used to examine the boride layer's adhesion characteristics. It has been reported that as boriding progresses, wear resistance rises and the friction coefficient falls.

In parts produced by the PM method, boriding is generally applied as a separate process after sintering. If the pack boriding technique is used while the powder compact is being sintered, sintering and boriding can be combined. This can save energy usage in addition to preventing parts from deforming as a result of secondary heating. Borosintering (BS) is the process of boriding the parts made using the PM method during the sintering process (Fang et a., 2020; Erdogan et al., 2020).

The borosintering process was used on iron-based samples that contained 0.4% C and 2% Cu by weight in Dong et al. (2009)'s investigation. 97% N_2 and 3% H_2 were present in the ambient during the processes, which were performed for four hours at a temperature between 1050 and 1150°C. The processing temperature caused the borided layers to vary in thickness from 63 to 208 µm. X-ray diffraction investigation verified the existence of Fe_2B and FeB phases in the structures of borided layers. According to certain reports, the microhardness values of borided layers range from 1360 to 2066 $HV_{0.3}$, which is significantly higher than the substrate material's hardness of about 186 $HV_{0.3}$. Based on the results of the wear test, it was found that as surface hardness increased, borided and sintered samples' wear resistance greatly improved. Erdogan et al. (2020) examined the sintering and borosintering properties of AISI 1010 (Fe−0.6Mn−0.4Si −0.1C) steel. The sintering process was applied in Al_2O_3 powder environment at 1000°C for 2 hours, and the borosintering process was applied in Ekabor 2 powder environment at 1000°C for 2, 4 and 6 hours. Depending on the sintering time and temperature, FeB+Fe_2B layer with a thickness of 120-400 µm was detected in the borosintered samples. Hardness was measured as 205−215 HV in sintered samples and 1252−1705 HV in borosintered samples. It has been stated that as the borosintering time increases, the hardness value increases but the wear resistance decreases. Iron-based material was borosinized for three, five, and ten hours at 850, 950, and 1050 degrees Celsius by Fang et al. (2020). It has been shown that the boride layer is mostly composed of a single phase that contains Fe_2B. It is uniformly thick and has a strong bond with the substrate. It has been reported that the layer's hardness and thickness progressively increase with temperature and time. It has been noted that an excessively thin or thick layer will result in a decrease in the bonding force between the substrate material and the layer. It was reported that boriding at 850 and 950°C produced a single-phase Fe_2B layer, and at 1050°C, a double-layer structure with FeB and Fe_2B phases was developed. Friction and wear testing have indicated that the boride layer has good wear resistance. Wear was shown to be produced by microcracks in boronized samples due to plastic deformation brought on by fatigue, and significant oxidation and

plastic deformation in non-borided samples. Koç (2020) examined the sintering and borosintering properties of AISI 1010 (Fe–0.6Mn–0.4Si–0.1C) steel. He stated that he pressed metal powders by cold pressing method at 1000 Psi pressure, used silicon powder as the sintering medium and EKabor 2 powder as the boronizing medium. In the samples subjected to borosintering, the coating thickness was measured as 120-150 µm and the microhardness was measured as 1300-1500 HV. It has been pointed out in the literature that boriding and sintering processes are carried out separately, and that when carried out in a single step, it has a positive effect on mechanical and wear properties. Turgut and Günen (2020) investigated the borosintering of Fe-1.75Ni-1.5Cu-0.5Mo steel, which is frequently used in automotive parts. In the study, sintering and borosintering processes were compared. The sintering process was carried out under a pure argon atmosphere, and the boriding process was carried out in an environment consisting of 90% B_4C + 10% $NaBF_4$ powder mixture. A FeB+Fe_2B layer with a thickness of 160-325 µm was detected in the borosintered samples. The hardness value was measured as 1405-1688 HV, and the elasticity modulus was measured as 122.21-162.42 GPa. In the samples sintered under argon atmosphere, the hardness value was measured as 215-250 HV and the elasticity modulus was measured as 63.28-94.86 GPa. It has also been stated that borosintered samples show superior corrosion resistance compared to conventional sintering.

In the literature, sintering and borosintering processes are generally compared. In this study, boriding of the samples was compared in two steps, first sintering and then boronizing, and in a single step (borosintering). In addition, a boronizing medium different from other studies (containing 20% B_4C, 75% SiC and 5% NaF powders with below 10 µm grain size) was used. In this context, it was aimed to obtain a lower surface roughness with fine-grained powder and to see the usability of the relatively more cost-effective NaF as an activator. A counter disc covered by 600 grit SiC sandpaper was used for the block-on-disc type wear test, which is a fairly typical method of conducting wear testing.

Materials and methods

Powder was prepared with 0.5% graphite, 0.2% silicon, 0.6% manganese, 0.6% zinc stearate and iron in balance for mechanical alloying process by Retsch PM100 planetary ball mill. The process was carried out using 5 mm diameter zirconium oxide balls for 90 minutes at 300 rpm. The prepared powder was pressed with 750 MPa pressure (84780 N) in a mold with a 12 mm internal diameter, made of AISI D2 material with a tolerance of 0.05 mm. To some of the pressed samples, sintering and boriding processes were applied simultaneously (i.e. borosintering) for 2 hours at temperatures of 950, 1000, 1050°C, and to some of them, first sintering (2 hours) and then boriding (2 hours) were applied separately at the same temperatures for total 4 hours.

In the boronizing environment, 20% B_4C (99% purity, 10 µm grain size), 5% NaF (99% purity), 75% SiC (99.1% purity, 1 µm grain size) powders were used as boron source, activator and filler, respectively. Boriding processes carried out with AISI 310 stainless steel box (100x100x50). Al_2O_3 powder (99.7% purity, 4.5 µm grain size) was used as deoxidant.

The sintering process of the samples, whose sintering processes were applied separately, was carried out in the MSE T_1600_70_450_(A) tube furnace, and the borosintering process and the boriding process applied after sintering were carried out in the Nabertherm chamber furnace. To ensure that the heating rates of both furnaces were the same, the control panel of the chamber furnace was recorded with a camera, and the heating rate was calculated with the data obtained from the recorded videos. In addition, the control panels of both furnaces were recorded during the heat treatment in order to calculate heating and cooling rates and to detect situations such as power cut (Figure 1).

Dust residues on the boronized and borosintered samples were cleaned first with a brush and then with acetone at room temperature in Isolab ultrasonic cleaner for 5 minutes. Some of the cleaned samples were cut and molding with bakelite. Molding samples were sanded with 120 – 2500 grit sandpaper and polished with 1 µm diamond solution. Metallographically prepared samples were examined with optical microscope and SEM, and microhardness measurements were made. XRD analysis, density measurement, surface roughness measurement and wear tests were performed on other samples that were not cut.

X-Ray Diffraction (XRD) analysis was performed to detect the phases formed as a result of boriding and borosintering processes in the samples. XRD analyzes were carried out using Cu Kα as the X-Ray source at speed of 1.5° min^{-1}.

Figure 1. Record panel of a) chamber furnace b) tube furnace with a camera.

Density measurement of the samples was carried out according to the Archimedes principle using an Axis AGN220C precision scale and an apparatus manufactured from a 3D printer. Surface roughness measurement was made from the lateral surfaces of the samples using a Taylor Hobson Surtronic 25 profilometer.

Wear tests were carried out with Plint TE 53 Multi-Purpose Friction and Wear Test Machine under 42, 62, 82 N loads for 200, 400, 600 m distance. A disc covered with 600 grit SiC sandpaper was used as the counter. The mass of the samples subjected to the wear test was weighed before and after the test, and the mass loss was determined. Friction force and displacement signals during the test were transferred to the computer via UART protocol using the Arduino nano development board and ADS 1115 16-Bit 4 Channel ADC. A program was written in Lazarus to calculate the friction coefficient from the received data and view the graphics instantly. The written program converts analog voltage signals into friction force and displacement by interpolation, and calculates the distance and friction coefficient using the entered speed, abrasive disc diameter and force. In addition, it provides their graphics instantly and allows them to be saved in csv format and processed later. Origin Pro Student Edition was used to process the received data (plot detailed graphs etc.).

Results and discussion

Average density calculated according to the Archimedes principle and the compactness ratio determined according to the theoretical density are given in Table 1. Compared to the sintered samples, the compactness ratio was calculated to be slightly lower in the sintered and boronized samples, and the lowest in the borosintered samples.

Table 1. Average density and compactness ratio of the samples.

Sample	Average Density [gr cm^{-3}]	Compactness Ratio [%]
Without heat treatment	7.179 ± 0.01	91.45 ± 0.12
Sintered at 950°C	7.202 ± 0.02	91.74 ± 0.20
Sintered and borided at 950°C	7.192 ± 0.01	91.62 ± 0.15
Borosintered at 950°C	7.077 ± 0.01	90.15 ± 0.15
Sintered at 1000°C	7.196 ± 0.01	91.67 ± 0.05
Sintered and borided at 1000°C	7.176 ± 0.01	91.41 ± 0.06
Borosintered at 1000°C	7.116 ± 0.01	90.65 ± 0.11
Sintered at 1050°C	7.188 ± 0.01	91.57 ± 0.13
Sintered and borided at 1050°C	7.144 ± 0.02	91.01 ± 0.29
Borosintered at 1050°C	7.059 ± 0.01	89.92 ± 0.15

Average surface roughness measured from the lateral surfaces of the samples are given in Table 2. It was observed that the surface roughness increased after sintering. Following the boriding process, the roughness values increased slightly, and the roughness values of the sintered and boronized samples and the borosintered samples were close to each other.

Table 2. Average Surface Roughness of the samples.

Sample	Average Surface Roughness		
	Ra	Rz	Rt
Without heat treatment	0.10 ± 0.01	0.80 ± 0.08	1.47 ± 0.31
Sintered at 950°C	0.41 ± 0.02	4.93 ± 0.57	11.53 ± 1.2
Sintered and borided at 950°C	1.31 ± 0.11	8.55 ± 0.95	12.15 ± 2.0
Borosintered at 950°C	1.39 ± 0.26	9.00 ± 1.5	13.35 ± 1.5
Sintered at 1000°C	0.44 ± 0.08	5.20 ± 1.3	8.07 ± 2.4
Sintered and borided at 1000°C	1.11 ± 0.08	7.67 ± 0.45	9.80 ± 1.1
Borosintered at 1000°C	1.31 ± 0.01	9.17 ± 0.78	11.83 ± 1.7
Sintered at 1050°C	0.55 ± 0.14	6.47 ± 1.9	9.33 ± 1.5
Sintered and borided at 1050°C	1.37 ± 0.23	7.50 ± 0.20	11.75 ± 2.3
Borosintered at 1050°C	1.27 ± 0.09	9.10 ± 1.1	13.33 ± 1.3

The temperature - time graph during heat treatment is given in Figure 2, and the average heating and cooling rates are given in Table 3. It can be seen that the temperature increase in the chamber furnace is parabolic, in the tube furnace it is linear, and the cooling occurs parabolically in both furnaces. However, it can be seen from the graphics that the tube furnace cools faster. The fact that the volume of the tube furnace is much smaller than the chamber type furnace and the continuous gas flow accelerates the cooling.

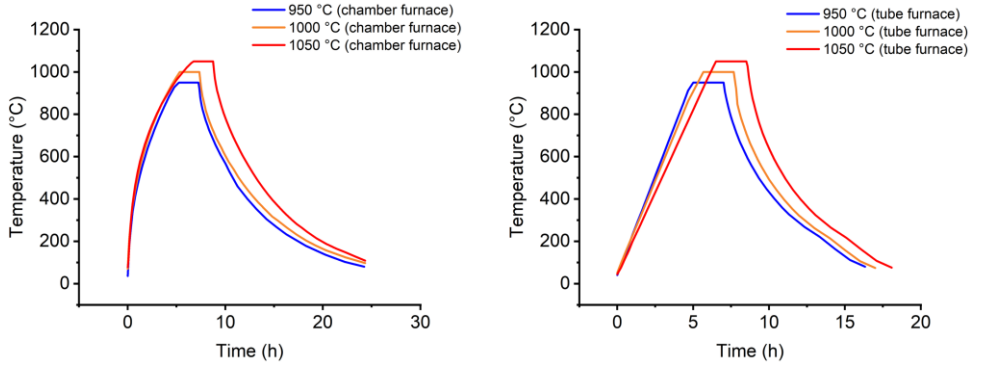

(a) **(b)**

Figure 2. Temperature – time graphs a) chamber furnace b) tube furnace.

Table 3. Heating and cooling rates during heat treatment.

Sample	Heating Rate (°C min^{-1}.)	Cooling Rate (°C min^{-1}.)
950°C (Tube Furnace)	3.104	3.037
950°C (Chamber Furnace)	2.901	1.957
1000°C (Tube Furnace)	2.881	3.269
1000°C (Chamber Furnace)	2.906	1.864
1050°C (Tube Furnace)	2.577	3.331
1050°C (Chamber Furnace)	2.400	1.919

Optical microscope images of sintered and borided samples and borosintered samples are given in Figure 3, and the average boride layer thicknesses (µm) obtained from the optical images are given in Table 4. It can be seen that the boride layer thickness increases depending on temperature and is saw-toothed. The layer thicknesses and morphologies of the sintered and boronized samples and the borosintered samples were similar.

Table 4. Average boride layer thicknesses.

Sample	Average boride layer thicknesses [µm]
Sintered and borided at 950°C	50.0 ± 7.9
Borosintered at 950°C	72.8 ± 9.7
Sintered and borided at 1000°C	95.7 ± 8.2
Borosintered at 1000°C	112.1 ± 8.5
Sintered and borided at 1050°C	167.0 ± 10.9
Borosintered at 1050°C	180.5 ± 10.9

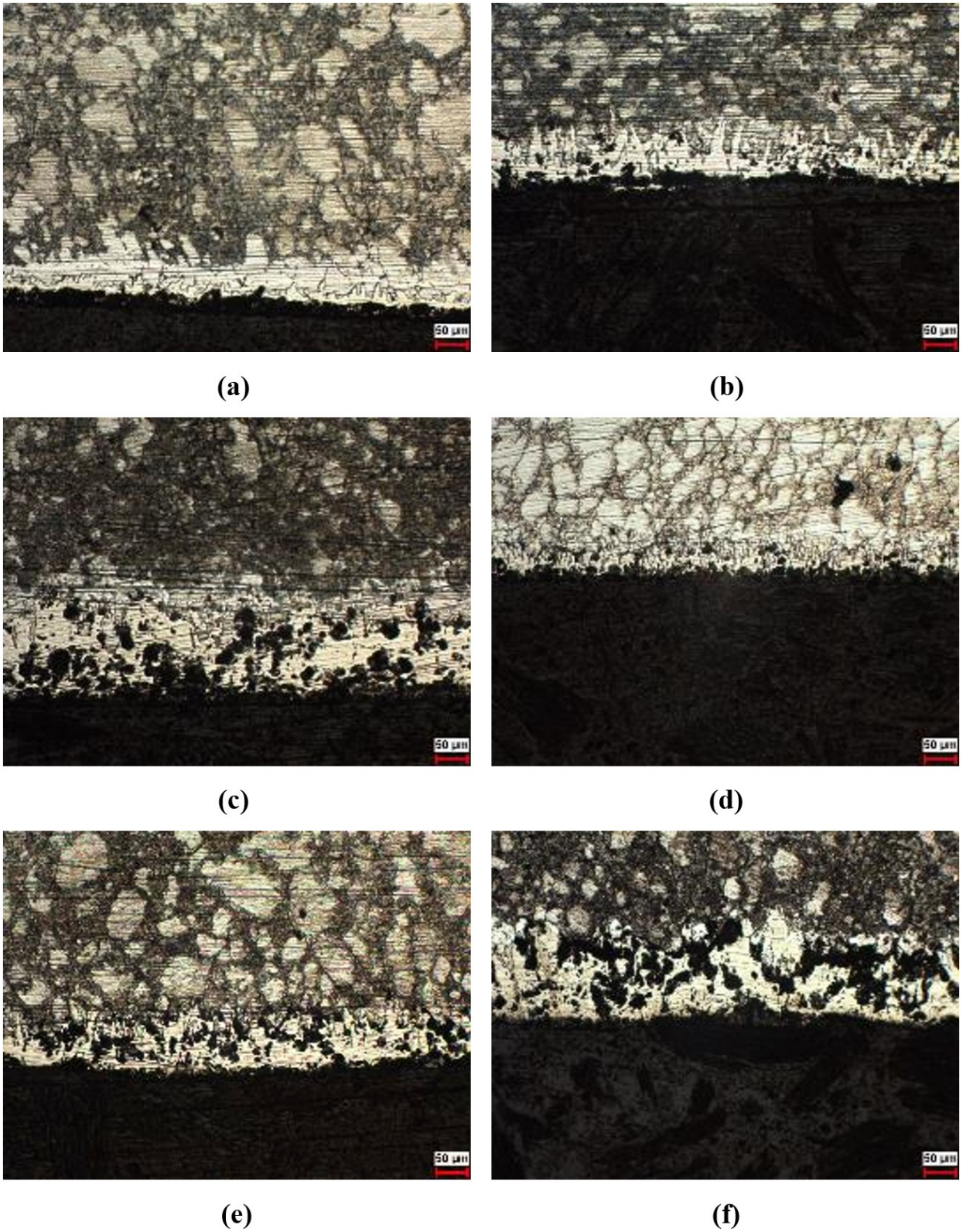

Figure 3. Optical microscope images of the sample sintered and borided at a) 950°C, b) 1000°C, c) 1050°C, borosintered at d) 950°C, e) 1000°C f) 1050°C.

SEM images and EDX elemental analyzes of sintered and boronized samples and borosintered samples are given in Figure 4. When looking at the color gradients, it is seen that the structure mostly consists of a single phase, and that there is a second boride phase, dense in terms of the amount of boron, that appears darker in some regions (especially in the outer regions of layers) (Figure 5). Micro cracks were seen in some regions (black points) of the boride layer. It can be said that some of these occur due to the brittleness of the boride layer during metallographic processes, and some of them arise from gaps during sintering.

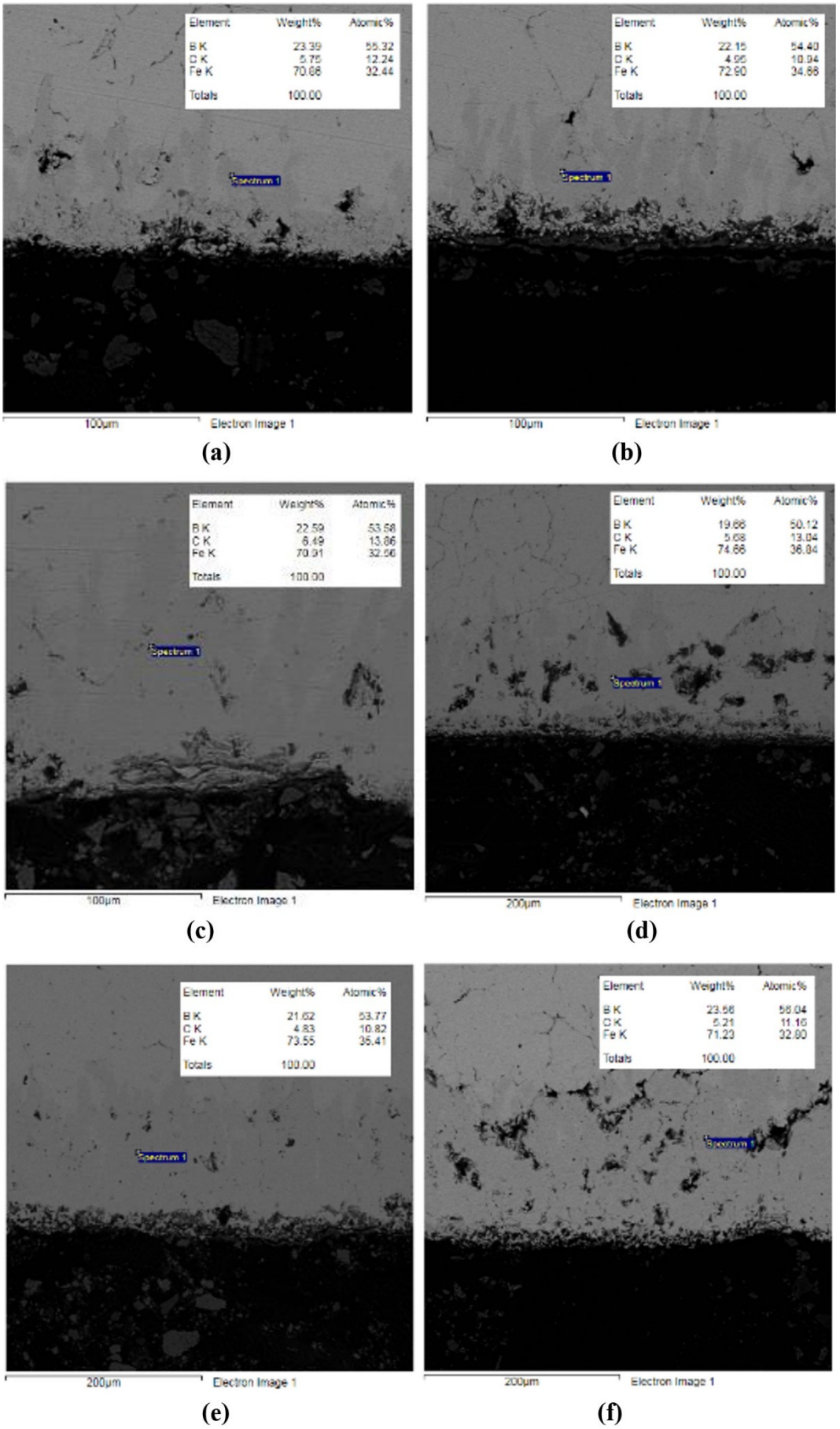

Figure 4. SEM images and EDX elemental analysis results of the sample sintered and borided at a) 950°C, b) 1000°C, c) 1050°C, borosintered at d) 950°C, e) 1000°C f) 1050°C.

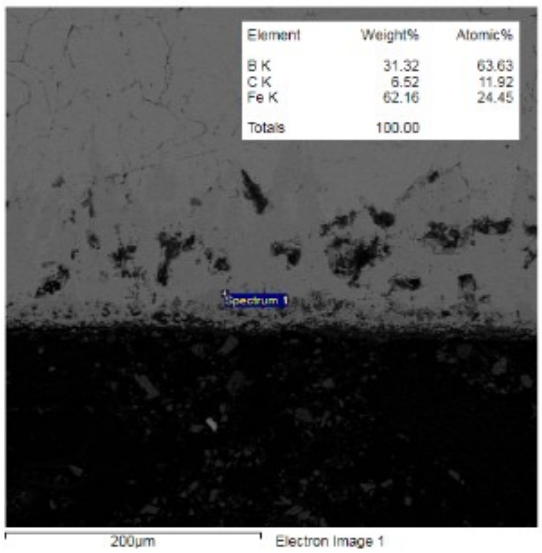

Figure 5. SEM images and EDX elemental analysis results of the boron-dense region of the sample borosintered at 1000°C.

Table 5 displays the findings of the microhardness measurement. Both the sintered samples and the borided samples exhibited similar microhardness values in the substrate. Regarding the boronized samples, at 1000 and 1050°C, the average hardness values in the boride layer were higher than those of the borided samples at 950°C. It is observed that boriding results in an enormous increase in the microhardness value.

Table 5. Microhardness measurement results.

Sample	Average Hardness [$HV_{0.05}$]	
	Boride Layer	Substrate
Sintered at 950°C	-	116 ± 8
Sintered and borided at 950°C	1490 ± 63	115 ± 15
Borosintered at 950°C	1472 ± 10	104 ± 12
Sintered at 1000°C	-	111 ± 12
Sintered and borided at 1000°C	1749 ± 51	114 ± 9
Borosintered at 1000°C	1699 ± 50	108 ± 8
Sintered at 1050°C	-	116 ± 10
Sintered and borided at1050°C	1757 ± 34	123 ± 12
Borosintered at 1050°C	1710 ± 43	122 ± 6

XRD spectrums of the samples are given in Figures 6, 7 and 8. When the spectra were examined, it was seen that the sintered sample consisted of Fe, and the boronized samples consisted mostly of Fe_2B. In examining the XRD spectrums, Crystal Impact Match! program has been used. Card numbers 96-901-3478 for Fe, 96-101-1337 for FeB and 96-151-1153 for Fe2B are referenced. In some samples boronized at 1000 and 1050°C, the FeB phase, similar to the Fe2B phase, was clearly seen. It can be said that this is caused by the concentration of FeB in the region where the sample was scanned in the XRD analysis. It was also detected in SEM and EDX analyzes that the FeB phase was concentrated in some regions of the samples.

Tables 6, 7, and 8 indicate the wear amounts, mass wear rates, average friction forces and coefficients, respectively. In order to better understand the increasing and decreasing trends, as an example, the results of the samples heat treated at 1000°C are given graphically in Figure 9, 10 depending on load and samples, recpectively. While the amount wear was high in the samples boronized at 950°C, it was significantly low in the samples borided at 1000 and 1050°C. This is because the boride layer formed at 950°C is very thin and the layer is wearing away in a short time and reaches the substrate material region. It has been observed that the amount of wear increases depending on the load and distance. In cases where the amount of wear did not increase much despite the increase in force, the mass wear rate did not change much (For example, the sample sintered and borided at 1050°C). In samples with low wear, the average friction force and friction coefficient were low in many samples. However, it is difficult to interpret the friction coefficient in some samples due to deviations caused by sudden load changes that occur from time to time. While the wear amount was high in the samples boronized at 950°C, it was significantly low in the samples borided at 1000 and 1050°C. It was seen that sintered and boronized samples and borosintered samples show similar wear characteristics (Figure 10).

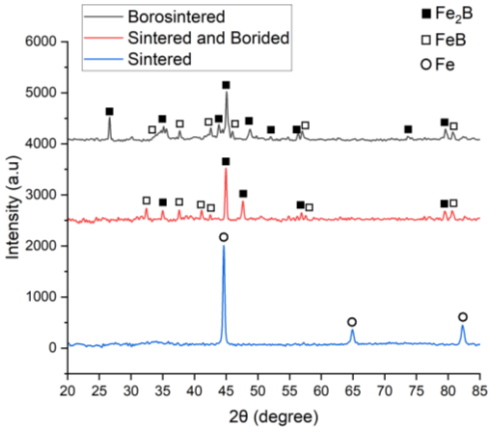

Figure 6. XRD spectrums of samples treated at 950°C.

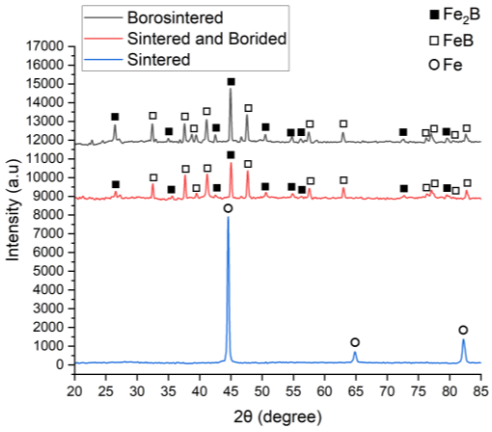

Figure 7. XRD spectrums of samples treated at 1000°C.

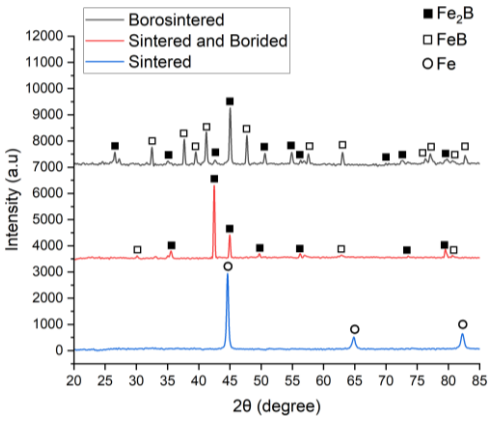

Figure 8. XRD spectrums of samples treated at 1050°C.

Table 6. Wear amounts of samples.

Distance [m]		200			400			600		
Load [N]		42	62	82	42	62	82	42	62	82
Sample		Wear amount [mg]								
S*	950°C	4.1	5.9	9.6	6.1	15.9	22.4	6.7	12.4	25.9
	1000°C	3.2	4.8	13.6	4.8	9.5	19.4	5.5	13.8	32.2
	1050°C	3.1	4.1	9.2	5.1	11.5	16.8	7.1	12.5	28
SB*	950°C	9.8	11.6	13.2	12.6	20.7	23.7	21.9	32	***
	1000°C	2.1	3.1	3.9	2.7	3.7	5	3.4	4.5	9.3
	1050°C	2.2	3.1	4.9	2.6	4	6.2	3	4.3	9.7
BS*	950°C	10	12.8	14.3	18.8	30.5	32.3	22.4	36.7	***
	1000°C	2.8	3.6	4.9	3	5.2	7.5	3.5	6.1	8.9
	1050°C	2.4	3	5.3	4	5.6	13	5.5	7.6	16.2

*S: Sintered SB: Sintered and Borided BS: Borosintered.

Table 7. Mass wear rates of samples.

Load [N]		42	62	82
Sample		Mass wear rate [mm³/Nm]		
S*	950°C	36.92	46.28	73.09
	1000°C	30.33	51.55	90.95
	1050°C	39.19	46.74	79.17
SB*	950°C	120.83	119.60	***
	1000°C	18.80	16.86	26.34
	1050°C	16.66	16.18	27.60
BS*	950°C	125.61	139.41	***
	1000°C	19.52	23.04	25.42
	1050°C	30.92	28.94	46.65

*S: Sintered SB: Sintered and Borided BS: Borosintered.

Table 8. Average friction force and coefficient of samples.

Load [N]		42	62	82	42	62	82
Sample		Friction Force [N]			Friction Coefficient [-]		
S*	950°C	13.864 ± 0.574	21.434 ± 0.668	28.470 ± 0.830	0.330 ± 0.014	0.346 ± 0.011	0.347 ± 0.010
	1000°C	11.448 ± 0.549	19.413 ± 0.750	29.872 ± 1.117	0.273 ± 0.013	0.313 ± 0.012	0.364 ± 0.014
	1050°C	10.021 ± 0.463	19.650 ± 0.763	28.200 ± 0.942	0.239 ± 0.011	0.317 ± 0.012	0.344 ± 0.011
SB*	950°C	12.445 ± 0.390	21.399 ± 0.924	27.284 ± 1.424	0.296 ± 0.009	0.345 ± 0.015	0.333 ± 0.017
	1000°C	10.106 ± 0.764	18.382 ± 1.284	26.700 ± 1.974	0.241 ± 0.018	0.296 ± 0.021	0.326 ± 0.024
	1050°C	7.892 ± 1.517	16.232 ± 0.970	23.384 ± 1.194	0.188 ± 0.036	0.262 ± 0.032	0.285 ± 0.015
BS*	950°C	12.160 ± 1.559	20.805 ± 2.172	31.783 ± 1.677	0.290 ± 0.037	0.336 ± 0.035	0.388 ± 0.020
	1000°C	10.402 ± 0.575	17.286 ± 0.980	22.881 ± 1.735	0.248 ± 0.014	0.279 ± 0.016	0.279 ± 0.021
	1050°C	9.630 ± 0.481	17.966 ± 0.682	26.154 ± 1.437	0.229 ± 0.011	0.290 ± 0.011	0.319 ± 0.018

*S: Sintered SB: Sintered and Borided BS: Borosintered.

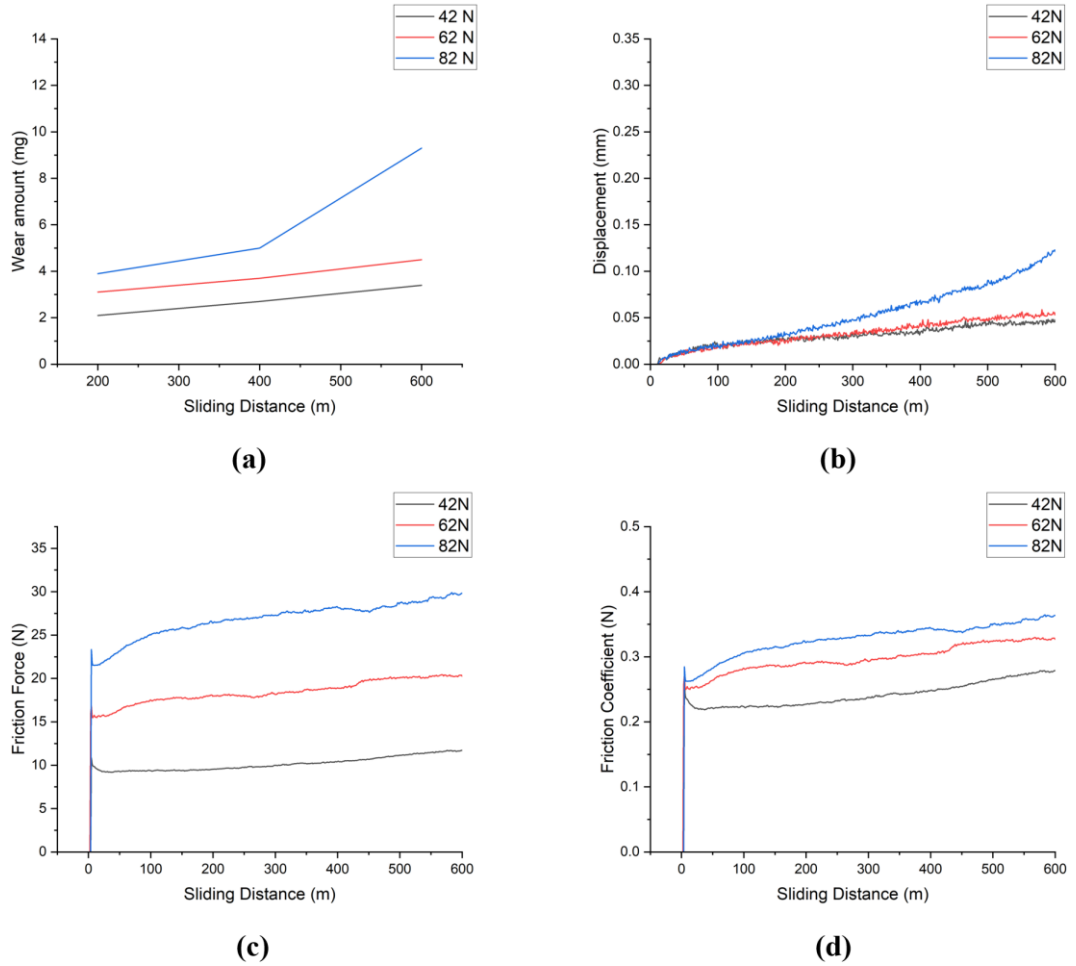

Figure 9. Wear depending on load of the sintered and borided sample at 1000°C a) wear amount b) displacement c) friction force d) friction coefficient

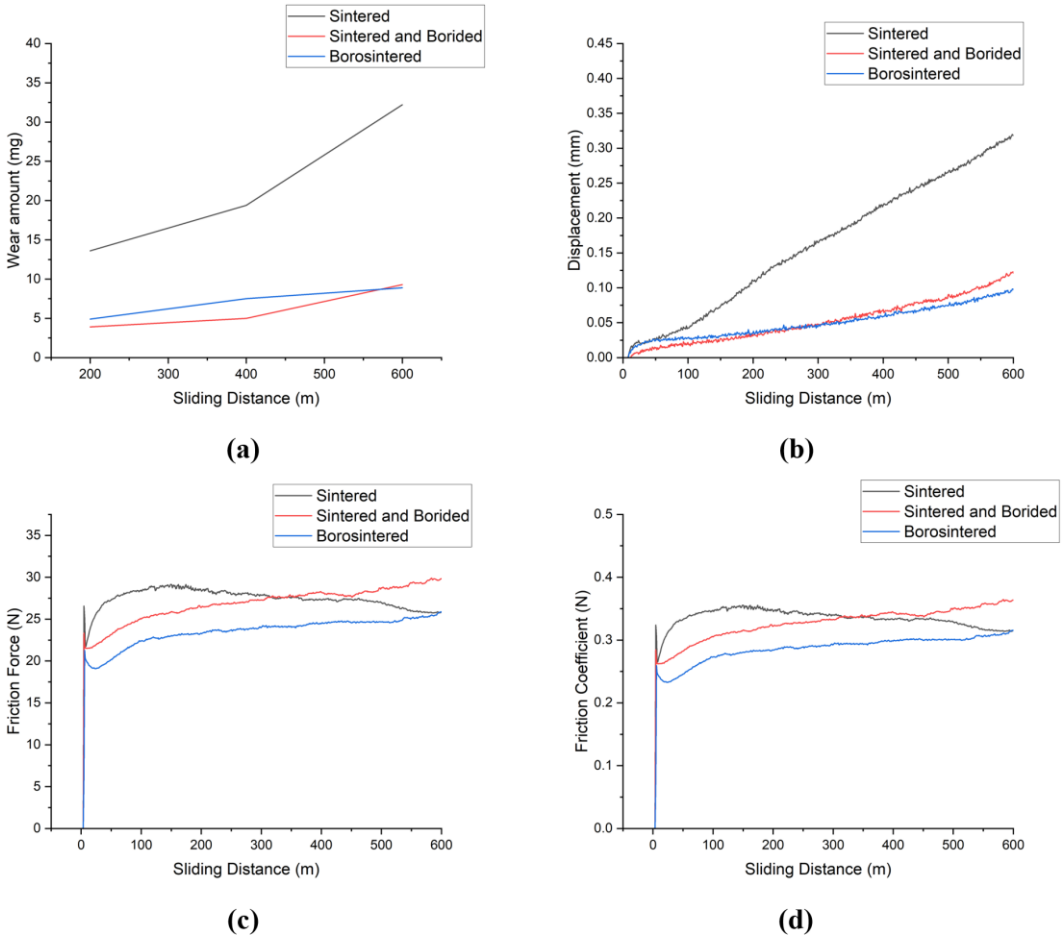

Figure 10. Wear depending on samples of the heat treated at 1000°C a) wear amount b) displacement c) friction force d) friction coefficient

Conclusion

Although the compactness ratio does not vary much in the samples, it is calculated to be slightly lower in the sintered and boronized samples compared to the sintered samples, and the lowest in the borosintered samples. In sintered and boronized samples, it can be said that the heat treatment for boriding after sintering may partially increase the porosity, which may reduce the compactness rate. It is thought that pores may form in borosinterned samples due to the diffusion of boron into the material during sintering.

It was observed that the surface roughness of the samples increased after sintering. After the boriding process, the roughness values of the samples increased slightly, and the roughness values of the sintered and boronized samples and the borosintered samples were close to each other. Since the surface quality of samples produced with powder metallurgy is close to perfect, surface roughness may increase slightly after heat treatments. Considering the average roughness value Ra (around 1.3 µm), it can be said that the surface roughness of the borided samples is quite low. It is thought that this is achieved by the fact that the boronizing medium consists of fine-grained powder.

Since the heating rate in the chamber furnace and tube furnace was optimized, they were close to each other at the same temperatures. The fact that the volume of the tube furnace is quite small compared to the chamber furnace and the continuous gas flow accelerates the cooling.

The boride layer thickness and morphology in the sintered and borided samples and the borosintered samples were close to each other. It was observed that the layer thickness increased with time. It has been observed that the layers generally consist of the Fe_2B phase, the amount of boron is concentrated regionally and the FeB phase is found in these regions. Boriding processes have been successfully carried out using the relatively cheaper NaF as the activator in the boriding environment.

It is observed that boriding results in a significant increase in the microhardness value. When comparing samples borided at 1000 and 1050°C to samples boronized at 950°C, the average hardness values in the boride layer of the former were greater.

Wear testing of high hardness boride layers could be carried out in a very traditional block-on-disc type wear test machine with a counter disc covered by 600 grit sandpaper, without the need for a new generation machine. While the amount wear was high in the samples boronized at 950°C, it was significantly low in the samples borided at 1000 and 1050°C. This is because the boride layer formed at 950°C is very thin and the layer is wearing away in a short time and reaches the substrate material region. Sintered and boronized samples and borosintered samples was shown similar wear properties.

As a result, the borosintering process and the traditional boriding process (sintering and boriding separately) are similar in many features. In both cases, many properties of the material are improved. The fact that the process steps in borosintering are few and that there is no need for an additional protective atmosphere such as Argon gas in iron-based materials reduces the cost considerably. For this reason, choosing the borosintering process in materials to be produced with powder metallurgy will provide a serious advantage. 1000 and 1050°C are more appropriate for boriding processes since wear tests show that the boride layer made at 950°C wears out quickly. If boriding is done in different boronizing environments at 950°C, layers with different morphologies may form. Additionally, slower wear can be achieved when different counter elements or parameters are used in wear tests.

References

Aksöz, S., Bostan, B., & Kaplan, Y. (2021). An Investigation on the Effects of Boronizing Process on Microstructure and Microhardness of NiTi Alloy Produced by P/M Technique. *Journal of Polytechnic*, *24*(2), 539–544. https://doi.org/10.2339/politeknik.717251

Altıntaş, A., Sarıgün, Y., & Çavdar, U. (2016). Effect of Ekabor 2 powder on the mechanical properties of pure iron powder metal compacts. *Revista de Metalurgia*, *52*(3), e073. https://doi.org/10.3989/revmetalm.073

Bouarour, B., Keddam, M., Allaoui, O., & Azouani, O. (2014). Boriding kinetics of C35 steel: estimation of boron activation energy and the mass gain. *Metallurgical Research & Technology*, *111*(2), 67–73. http://doi.org/10.1051/metal/2014015

Çavdar, U., Ünlü, B. S., Pınar, A. M., & Atík, E. (2015). Mechanical properties of heat treated iron based compacts. *Materials in Engineering*, *65*, 312–317. https://doi.org/10.1016/j.matdes.2014.09.015

De Almeida, E. A. dos S., Krelling, A. P., Milan, J. C. G., & da Costa, C. E. (2018). Micro-abrasive wear mechanisms of P/M AISI M2 steel with different surface treatments. *Surface and Coatings Technology*, *333*, 238–246. https://doi.org/10.1016/j.surfcoat.2017.10.020

Dong, X., Hu, J., Huang, Z., Wang, H., Gao, R., & Guo, Z. (2009). Microstructure and properties of boronizing layer of Fe-based powder metallurgy compacts prepared by boronizing and sintering simultaneously. *Science of Sintering*, *41*(2), 199–207. https://doi.org/10.2298/SOS0902199D

Erdogan, A., Kursuncu, B., Günen, A., Kalkandelen, M., & Gok, M. S. (2020). A new approach to sintering and boriding of steels "Boro-sintering": Formation, microstructure and wear behaviors. *Surface and Coatings Technology*, *386*(February), 125482. https://doi.org/10.1016/j.surfcoat.2020.125482

Fang, H., Xu, F., & Zhang, G. (2020). Investigation of Dry Sliding Wear Behavior of Pack Boriding Fe-Based Powder Metallurgy. *Integrated Ferroelectrics*, *208*(1), 67–82. https://doi.org/10.1080/10584587.2020.1728717

Kare, D., Shoba, C., Dora, S. P., & Swain, P. K. (2021). Damping characteristics of pure aluminum: A comparison of microwave and conventional sintering. *Metal Powder Report*, *76*(6), 22–25. https://doi.org/10.1016/s0026-0657(21)00299-x

Kayalı, Y., & Yönetken, A. (2021). Investigation of Wear Behavior of Borided Materials Produced by the Powder Metallurgy Method in Different Compositions. *Protection of Metals and Physical Chemistry of Surfaces*, *57*(4), 771–778. https://doi.org/10.1134/S2070205121040122

Keddam, M., & Chentouf, S. M. (2005). A diffusion model for describing the bilayer growth (FeB/Fe2B) during the iron powder-pack boriding. *Applied Surface Science*, *252*(1), 393–399. https://doi.org/10.1016/j.apsusc.2005.01.016

Koç, V. (2020). Effect of boro-sintering process on mechanical properties and wear behaviour of low alloy steel produced by powder metallurgy. *Materials Research Express*, *6*(12), 1265c3. https://doi.org/10.1088/2053-1591/ab636b

Ozbek, I., & Bindal, C. (2002). Mechanical properties of boronized AISI W4 steel. *Surface and Coatings Technology*, *154*(1-4), 13-17. https://doi.org/10.1016/s0257-8972(01)01409-8

Özdemir, O., Omar, M. A., Usta, M., Zeytin, S., Bindal, C., & Üçışık, A. H. (2009). An investigation on boriding kinetics of AISI 316 stainless steel. *Vacuum*, *83*(1), 175–179. https://doi.org/10.1016/j.vacuum.2008.03.026

Šalak, A., Selecka, M., Vasilko, K., & Danninger, H. (2008). Face Turning of PM Steels: Effect of Porosity and Carbon Level. *International Journal of Powder Metallurgy*, *44*(3), 49–61.

Sinha, A. K. (1991). Boriding. *Journal of Heat Treating*, *4*(4), 437–447.

Turgut, S., & Günen, A. (2020). Mechanical Properties and Corrosion Resistance of Borosintered Distaloy Steels. *Journal of Materials Engineering and Performance*, *29*(11), 6997–7010. https://doi.org/10.1007/s11665-020-05186-x

Yılmaz, S. S., & Varol, R. (2010). The effect of surface hardening treatments on the mechanical properties of iron based P/M specimens. *Powder Technology*, *204*(2–3), 236–240. https://doi.org/10.1016/j.powtec.2010.08.007